



The Effect of Strong Magnetic Field on Heavy Quarkonia in a Hot Medium using Nikiforov-Uvarov Method

M. Abu-shady^{1*} and H. M. Fath-Allah²

¹Department of Mathematics and Computer Sciences, Faculty of Science, Menoufia University, Egypt.

²Higher Institute of Engineering and Technology, Menoufia, Egypt.

Abstract

The influence of temperature and a constant strong magnetic field on quarkonium heavy meson spectrum is explored as a result of recent research suggesting that a strong magnetic field can be formed at primary stage in ultra relativistic heavy ion collisions (URHIC). Debye screen potential is used in non-relativistic models, and the states are termed as charmonium & bottomonium. In order to better understand the current findings, a comparison has been made in recent studies. Therefore, the number of flavor and magnetic field play an essential role in hot medium.



Article History

Received: 13 October 2021

Accepted: 26 November 2021

Keywords

Finite Temperature;
N-Dimensional Radial Schro'Dinger Equation;
Nikiforov Uvarov Method;
Strong Magnetic Field.

Introduction

In the mid- seventies, scientists investigated the possibility of quark-gluon plasma (QGP).^{1,2} The URHIC events have recently been reported when the magnetic field effect is combined with an exceptionally strong magnetic field.³⁻⁷ The strength of the magnetic field is dependent on the centrality and could be between $m_{\pi}^2 (\approx 10^{18} \text{ Gauss})$ at RHIC⁸ to $10 m_{\pi}^2$ at LHC.¹ It is capable of achieving levels of in extreme situations. $50m_{\pi}^2$ The Higgs field gradients rendered an extraordinarily

enormous magnetic field ($\sim 10^{23} \text{ Gauss}$), during the electroweak stage transition in the early cosmos.⁹

The dissociation of quarkonia necessitates the measuring of heavy quarkonium potentials in a disordered manner.^{10,11-13} Over the last two decades, the dynamics the dissociation of quarkonium have been seen in a medium where, in the beginning the resonance was assumed to be dissociated if screening is robust enough, i.e. potential is too small to keep pair appointed by $Q\bar{Q}$. Dissociation

CONTACT M. Abu-shady ✉ dr.abushady@gmail.com 📍 Department of Mathematics and Computer Sciences, Faculty of Science, Menoufia University, Egypt.



© 2021 The Author(s). Published by Oriental Scientific Publishing Company

This is an Open Access article licensed under a Creative Commons license: Attribution 4.0 International (CC-BY).

Doi: <http://dx.doi.org/10.13005/OJPS06.01-02.04>



is currently considered primarily to be due to the increase in the resonance distance either due to an inelastic mechanism of spatially mediated dispersion by a patron such as gluons, known as Landau damping¹⁴ or because of a process glue-dissociation in which involves hard thermal gluon in one-tone color state.¹⁵ In several approach models, the effect of eB on QCD thermo-dynamics has been examined.¹⁶⁻³⁸

A few studies have looked into the effect of magnetic fields on the static characteristics of quarkonium.^{10,39-45} One of the study influences on the features of nuclear matter under extreme settings has been heavy quarkonia. as quarkonia form in URHICs field as at a very period of $\sim 1/2m_Q$ (where m_Q is mass of charm or bottom quark), this is equivalent to time scale at which magnetic field is produced. In presence of an external magnetic field, vacuum quantum with harmonic oscillators and Cornell potential^{39,42} were recently mechanically investigated with quarkonium and heavy meson spectroscopy, with an additional spin-spin interaction component. The effect of finite T and eB on the real part of $Q\bar{Q}$ potential in form of destructive thermal QCD & dissociation of heavy quarkonia due to color screening have been studied.⁴⁶ In Ref.,¹⁶ the real part of potential is included in SE in order to determine energy eigenvalues and energy eigen functions of the states of the $c\bar{c}$. On the other hand, the magnetic field plays an important in the non-fluid mechanics such as in Refs.⁶⁰⁻⁶³

The aim of the present work, we have analytically solved Schrödinger equation using NU method in which the finite temperature and magnetic field are included in the potential interaction. For our best knowledge, the previous works are not solved the present potential analytically. In addition, the effect of number of flavors is studied on binding energy and dissociation temperature of quarkonium.

This paper is organized as follows. In Sec. 2, we describe NU method. In Sec. 3, the method is used to solve N-dimensional SE. In Sec. 4, we discuss the results, and summary & conclusion are given in Sec.5.

Theoretical Method

The NU method⁴⁷ used to solve the second-order differential equation in form is defined as follows

$$\Psi''(s) + \frac{\bar{\tau}(s)}{\sigma(s)} \Psi'(s) + \frac{\sigma(s)}{\sigma^2} \Psi(s) = 0, \quad \dots(1)$$

where $\bar{\sigma}$ and $\sigma(s)$ are max-second degree polynomials and $\bar{\tau}(s)$ is the first degree maximal polynomials. By using the transformation of $s = s(r)$,

$$\Psi(s) = \Phi(s) x(s), \quad \dots(2)$$

as in Ref.⁴⁸, Eq. (1) can be written

$$\sigma(s)x''(s) + \tau(s)x'(s) + \lambda x(s) = 0, \quad \dots(3)$$

where,

$$\sigma(s) = \pi(s) \frac{\Phi(s)}{\Phi'(s)}, \quad \dots(4)$$

where, $\pi(s)$ are the first degree polynomial⁴⁷ and

$$\tau(s) = \bar{\tau}(s) + 2 \pi(s); \quad \bar{\tau}'(s) < 0, \quad \dots(5)$$

then, the new eigenvalue equation becomes

$$\lambda = \lambda_n = -n \tau'(s) - \frac{n(n-1)}{2} \sigma''(s), \quad n = 0,1,2, \quad \dots(6)$$

$x(s) = x_n(s)$ is an n degree polynomial which fulfils the form of the Rodrigues

$$x_n(s) = \frac{B_n}{\rho_n} \frac{d^n}{ds^n} (\sigma''(s) \rho(s)), \quad \dots(7)$$

where B_n is a constant of normalization and $\rho(s)$ is a function of weight that follows the next equation

$$\frac{d}{ds} \omega(s) = \frac{\tau(s)}{\sigma(s)} \omega(s), \quad \omega(s) = \sigma(s) \rho(s), \quad \dots(8)$$

$$\pi(s) = \frac{\sigma'(s) - \bar{\tau}(s)}{2} \pm \sqrt{\left(\frac{\sigma'(s) - \bar{\tau}(s)}{2}\right)^2 - \check{\sigma}(s) + K \sigma(s)}, \quad \dots(9)$$

and

$$\lambda = K + \pi'(s) \quad \dots(10)$$

$\pi(s)$ is a first degree polynomial. The K in square-root of Eq. (9) is possible to determine whether expression under square root is square of expression. This is possible if the discrimination is zero.

The Solution of the Schrödinger Equation in the Presence of a Strong Magnetic Field.

As in Ref.⁴⁹, in N-dimensional space, the Schrödinger equation for two particles which interact with symmetrical potentials takes form

$$\left[\frac{d^2}{dr^2} + \frac{N-1}{r} \frac{d}{dr} - \frac{l(l+N-2)}{r^2} + 2\mu (E - V(r))\right]\Psi(r) = 0, \quad \dots(11)$$

Where l , N & μ are angular momentum quantum number, dimensional number, & reduced mass. Following radial SE is obtained by applying the wave function $\Psi(r) = r^{\frac{1-N}{2}} R(r)$

$$\left[\frac{d^2}{dr^2} + 2\mu (E - V(r) - \frac{(l+\frac{N-2}{2})^2 - 1}{2\mu r^2})\right]R(r) = 0. \quad \dots(12)$$

In the present work, the radial Schrödinger equation is employed which means potential interaction is symmetry. So, the potential takes following form as in Ref.⁵⁰ This potential depends on the radial distance. The effect of magnetic field will be appearing through the Debye mass. In addition, the anisotropy in the present potential with respect to the direction of magnetic field is not breaks the translational invariance of space, (for detail, see Ref.⁴⁶).

$$V(r) = \frac{-4}{3} \alpha \left(\frac{e^{-m_D r}}{r} + m_D\right) + \frac{4}{3} \frac{\sigma}{m_D} (1 - e^{-m_D r}), \quad \dots(13)$$

where,

the string tension $\sigma = 0.18 \text{ GeV}^2$ in Ref.¹⁶

$$\alpha = \frac{12 \pi}{11 N_c \ln\left(\frac{\mu_0^2 + M_B^2}{\Lambda_V^2}\right)} \quad \dots(14)$$

where,

N_c is the number of colors, M_B ($\sim 1 \text{ GeV}$) is an infrared mass which is interpreted as the ground state mass of the two gluons bound to by the basic string, $\mu_0 = 1.1 \text{ (GeV)}$, $\Lambda_V = 0.385 \text{ (GeV)}$ as in Refs.⁵¹⁻⁵³ and the Debye mass⁵³ becomes

$$m_D^2 = g^2 T^2 + \frac{g^2}{4\pi^2 T} \sum_f |q_f B| \int_0^\infty \frac{e^\beta \sqrt{p_z^2 + m_f^2}}{(1 + e^\beta \sqrt{p_z^2 + m_f^2})^2} dp_z, \quad \dots(15)$$

where,

the first term is the contribution from the gluon loops and dependent on temperature and the magnetic field doesn't affect it. The second term is this term strongly depends on the eB and is not much sensitive to the T of the medium. In the first term, where g is the running strong coupling and is given by

$$g = 4 \pi \hat{\alpha}_s (T), \quad \dots(16)$$

where,

$\hat{\alpha}_s (T)$ is the usual temperature-dependent running coupling. It is given by

$$\hat{\alpha}_s (T) = \frac{2 \pi}{\left(11 - \frac{2}{3} N_f\right) \ln\left(\frac{\Lambda}{\Lambda_{QCD}}\right)}. \quad \dots(17)$$

where,

N_f is the number of flavors, Λ is the renormalization scale is taken as $2 \pi T$ and $\Lambda_{QCD} \sim 0.2 \text{ (GeV)}$ as in Ref.¹⁶

The second term is $g = 3.3$, q_f is the quark flavor $f = u$ and d , B is the magnetic field, β is the inverse of temperature and quark mass massive $m_f = 0.307 \text{ (GeV)}$ as in Ref.⁵⁴ In Eq. (13), $e^{-m_D r}$ is expanded up to second-order where $m_D r \ll 1$ is considered as in.⁵⁵ Eq. (13) is written as follows

$$V(r) = a_1 r^2 + a_2 r + \frac{a_3}{r} \quad \dots(18)$$

where,

$$a_1 = \frac{-2}{3} \sigma m_D, \quad \dots(19)$$

$$a_2 = \frac{-4}{3} \alpha m_D^2 + \frac{4}{3} \sigma, \quad \dots(20)$$

$$a_3 = \frac{-4}{3} \alpha. \quad \dots(21)$$

By substituting the Eq. (18) into the Eq. (12), we get

$$\left[\frac{d^2}{dr^2} + 2\mu (E - a_1 r^2 - a_2 r - \frac{a_3}{r} - \frac{(l+\frac{N-2}{2})^2 - 1}{2\mu r^2})\right]R(r) = 0, \quad \dots(22)$$

By using $r=1/x$ and r_0 is the characteristic meson radius. So we could rewrite the Eq. (22) as in Ref.⁵⁶

$$\left[\frac{d^2}{dx^2} + \frac{4x}{x^2} \frac{d}{dx} + \frac{2\mu}{x^4} (E - \frac{a_1}{x^2} - \frac{a_2}{x} - a_3 x - \frac{(l+\frac{N-2}{2})^2 - 1}{2\mu} x^2)\right]R(x) = 0, \quad \dots(23)$$

The scheme is then based on $1/x$ extensions r_0 , $y=x-\delta$ and power series around $y=0$ where δ is a free parameter. Then, we have the scheme

$$\frac{1}{x} = \frac{1}{y+\delta} = \frac{1}{\delta} \left(1 + \frac{y}{\delta}\right)^{-1} \approx \frac{3}{\delta} - \frac{3x}{\delta^2} + \frac{x^2}{\delta^3}, \quad \dots(24a)$$

$$\frac{1}{x^2} = \frac{1}{(y+\delta)^2} = \frac{1}{\delta^2} \left(1 + \frac{y}{\delta}\right)^{-2} \approx \frac{6}{\delta^2} - \frac{8x}{\delta^3} + \frac{3x^2}{\delta^4}, \quad \dots(24b)$$

Substituting Eqs. (24) into Eq. (23), we get

$$\left[\frac{d^2}{dx^2} + \frac{4x}{x^2} \frac{d}{dx} + \frac{2}{x^4} (-A_1 + B_1 x - C_1 x^2)\right]R(x) = 0, \quad \dots(25)$$

where,

$$A_1 = -\mu \left(E - \frac{6 a_1}{\delta^2} - \frac{3 a_2}{\delta} \right), \quad \dots(26)$$

$$B_1 = \mu \left(\frac{8 a_1}{\delta^3} + \frac{3 a_2}{\delta^2} - a_3 \right), \quad \dots(27)$$

$$C_1 = \mu \left(\frac{3 a_1}{\delta^4} + \frac{a_2}{\delta^3} + \frac{(l + \frac{N-2}{2})^2 - \frac{1}{4}}{2 \mu} \right). \quad \dots(28)$$

By comparing Eq. (25) and Eq.(1), we obtain $\bar{\tau}(s) = 4x$, $\sigma(s)=x^2$ and $\check{\sigma}(s) = 2(-A_1+B_1x - C_1x^2)$. Hence, Eq. (25) fulfils Eq. (1), therefore, the following NU method as in Sec. 2,

$$\pi = -x \pm \sqrt{-2B_1 + 2A_1(1 + K + 2 C_1)x^2} \quad \dots(29)$$

Constant K is selected as it has a double zero under the square root, i.e. its discriminant $\Delta = 4B_1 - 8 A_1(1+K+2 C_1) = 0$. Hence,

$$\pi = -x \pm \frac{1}{\sqrt{2A_1}} (2A_1 - B_1x). \quad \dots(30)$$

Thus,

$$\tau = 4x \pm 2(-x + \frac{1}{\sqrt{2A_1}} (2 A_1 - B_1x)). \quad \dots(31)$$

In the above equation, we select the positive sign to have a derivative

$$\tau' = 2 - \frac{2B_1}{\sqrt{2 A_1}} \quad \dots(32)$$

using the Eq. (10), we get

$$\lambda = \frac{B_1^2}{2 A_1} - 2 C_1 - \frac{B_1}{\sqrt{2 A_1}} - 2 \quad \dots(33)$$

and Eq. (6), we obtain

$$\lambda_n = -n \left(2 - \frac{2 B_1}{\sqrt{2 A_1}} \right) - n(n-1) \quad \dots(34)$$

From Eq. (6), $\lambda = \lambda_n$.

$$\frac{B_1^2}{2 A_1} - 2 C_1 - \frac{B_1}{\sqrt{2 A_1}} - 2 = -n \left(2 - \frac{2 B_1}{\sqrt{2 A_1}} \right) - n(n-1) \quad \dots(35)$$

Let, $z = B_1/\sqrt{2 A_1}$ then the equation becomes quadratic

$$z^2 - (2n+1)z + (n^2 + n - 2(C_1 + 1)) = 0 \quad \dots(36)$$

The Eq. (36) is solved, we get the spectrum of energy

$$E = \frac{6 a_1}{\delta^2} + \frac{3 a_2}{\delta} - \frac{2 \mu \left(\frac{3 a_1}{\delta^3} + \frac{3 a_2}{\delta^2} - a_3 \right)^2}{\left[(2n+1) \pm \sqrt{1 + 8 \mu \left(\frac{3 a_1}{\delta^4} + \frac{a_2}{\delta^3} + \frac{(l + \frac{N-2}{2})^2 - \frac{1}{4}}{2 \mu} \right)} \right]^2} \quad \dots(37)$$

Results and Discussion

We note that Debye screening depends on eB and T . In Fig. (1), we find m_D increases with the temperature linearly and the effect the N_f plays a role in increasing the Debye mass with temperature. In the left panel, when $m_f > T$ and $T^2 < eB$, the Debye mass increases with temperature. In right panel, when $m_f < T$ and $T^2 < eB$, the Debye mass increases with temperature and we note that the quark mass does not affect on the Debye mass. This conclusion is in an agreement with Ref.⁵⁷

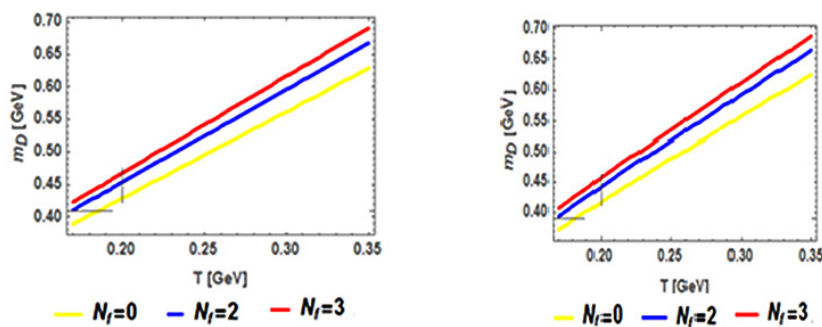


Fig. 1 : Left panel: Debye mass is plotted with T for different values the number of flavors at a fixed value of B ($eB=10 m_\pi^2$) and quark mass ($m_f=0.307$ GeV). Right panel: the Debye mass is plotted for the different values of the number of flavors at a fixed value of B ($eB=10 m_\pi^2$) and quark masses ($m_f=0.025$ (GeV).

In Fig. (2), we note that m_D increases with T and increases the number of flavors. In left panel, when $m_f > T$, $T^2 < eB$, the Debye mass increases with increasing temperature. In the right panel, when $m_f < T$ and $T^2 < eB$, the Debye mass increases with

increases to temperature. Therefore, we noted that increasing magnetic field up to $15 m_\pi^2$ is not affected on the behavior of the Debye mass. Also, this conclusion is an agreement with Ref. [16].

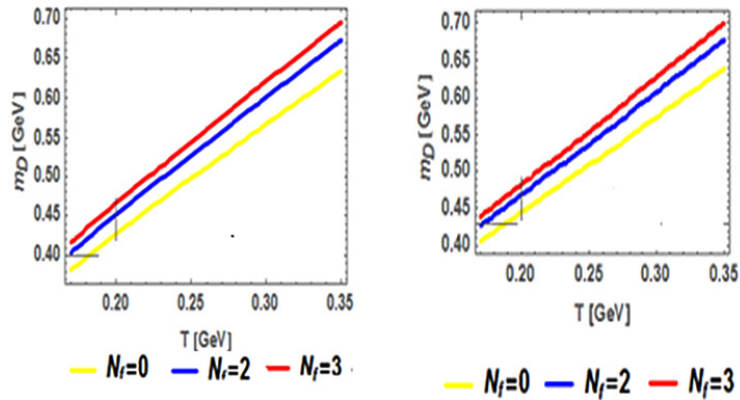


Fig. 2: Left panel: the screening Debye mass is plotted as function of T for different the number of flavors at a fixed value of $B(eB=15 \text{ m}\pi^2)$ and quark masses ($m_f=0.307(\text{GeV})$). Right panel: the Debye screening mass with T for different values of the number of flavors at a fixed value of $B eB=15 \text{ m}\pi^2$ and quark masses ($m_f=0.025(\text{GeV})$).

In Fig. (3), in the left panel the m_D increases with increasing T and eB with ($N_f=2$) and quark masses massive ($m_f=0.307(\text{GeV})$). We show that the m_D increases linearly both with T & eB . We took quark masses mass ($m_f=0.025(\text{GeV})$). In the

right panel, we have plotted Debye screening mass with temperature and magnetic field B with ($N_f=2$), we find that the quark mass does not affect on the Debye mass.

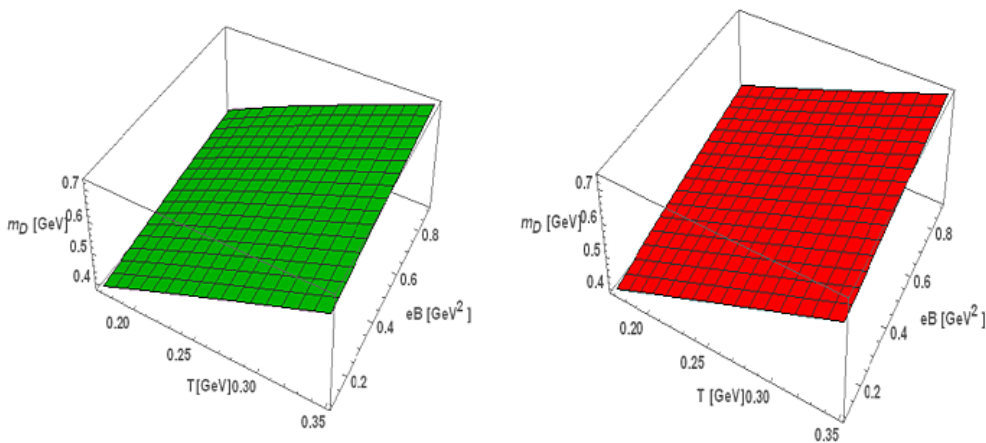


Fig. 3: In the left panel the Debye screening mass is plotted with temperature and magnetic field B at ($N_f=2$) and quark masses ($m_f=0.307(\text{GeV})$). In the right panel, Debye screening mass is plotted with temperature and magnetic field B at ($N_f=2$) and quark masses ($m_f=0.025(\text{GeV})$).

In Fig.(4), we have plotted Debye screening mass with temperature and magnetic field B with ($N_f=0, N_f=2$) and quark masses ($m_f=0.307(\text{GeV})$). We show that the m_D increases linearly with both T and eB . By increasing the number of flavors, the Debye mass increases with temperature and magnetic field.

Also, in this section, we note compartment of real potential that shows fundamental role in current work. Quark-antiquark interaction potential is plotted a function of distance (r), where the T and eB is included in the potential through the m_D . The Debye screening mass is parameterized according to Eq. (15) in which $N_c = 3, N_f=2$ and $g = 3.3$ are taken.

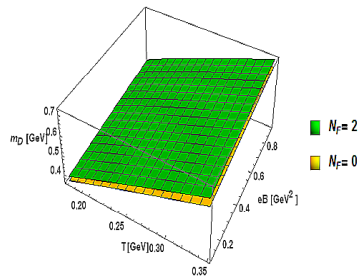


Fig. 4: The Debye screening mass is plotted with temperature and magnetic field B at ($N_f=0, N_f=2$) and quark masses ($m_f=0.307(\text{GeV})$).

In Fig. (5), in the left panel, we plotted real part of potential as a function of r for different values of the magnetic field like $eB=10 m_\pi^2, eB=25m_\pi^2$

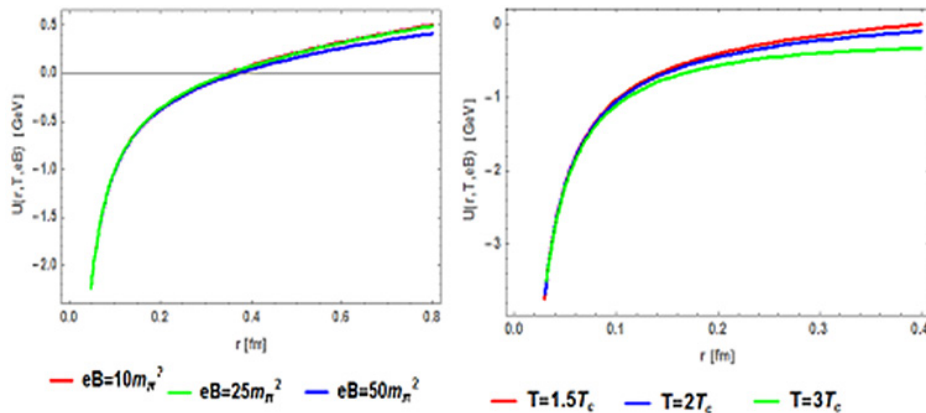


Fig. 5: Potential interaction is plotted as a distance function (r) for different magnetic field values. In the right panel, the potential interaction is plotted as a distance function (r) for different potential temperature values.

In Fig. (6), we have plotted real part of potential as function of the temperature and the magnetic field for the fixed value of $r = 0.2 \text{ fm}$. To see the change of the potential with the strong magnetic field for the temperature range $T= 0.17- 0.3 \text{ GeV}$, we notice that potential is more attractive with a magnetic field than temperature. This conclusion is in agreement with.⁵⁸

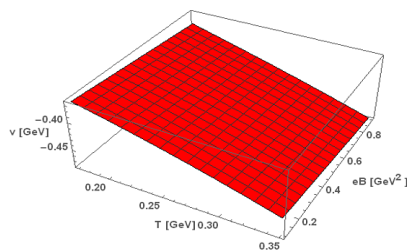


Fig. 6: Effect the temperature and magnetic field on the potential.

and $eB=50m_\pi^2$ at the fixed value of temperature $T=T_c$. We noted that when value of eB is increased the real-part is more screened. We noted that the ($eB=10m_\pi^2$) has an effect on the linear term. However, a further increase of magnetic field ($eB=25m_\pi^2$) and ($eB=50m_\pi^2$) the potential becomes more attractive than $eB=10m_\pi^2$. In the right panel, we have plotted real part of potential as function of different temperature values like $T=1.5 T_c, T=2 T_c$, and $T=3 T_c$ for a fixed value of $eB=10 m_\pi^2$. We have seen that the potential is screened by increasing the temperature. As a result, the real part of potential was found to be more screened to increase value of both T & eB . This conclusion has been agreed with Ref.¹⁶

Binding Energy

By solving Schrodinger equation as discussed in Sec. 3. We need to mention that the radial Schrödinger equation is numerically solved as in Refs.^{46, 50} We obtain the BEs of $c\bar{c}$ and $b\bar{b}$. In following, we see the change of the binding energy under the effect of temperature and magnetic field.

Charmonium binding energy is plotted as a function of T for three cases $eB=5 m_\pi^2, eB=25m_\pi^2$ and $eB= 50m_\pi^2$. In Fig. (7), we show the effect of the eB , temperature, and number of flavors on the BE of charmonium. We find that the BEs decreases with increasing T and magnetic field decrease. Besides, we have seen that the effect of temperature is more effective than the extremal magnetic field.

This conclusion is in an agreement with works^{16,50} Also, the binding energy decreases with increasing

number of flavors (N_f) as shown in Fig. (7). The effect is not considered in other works.

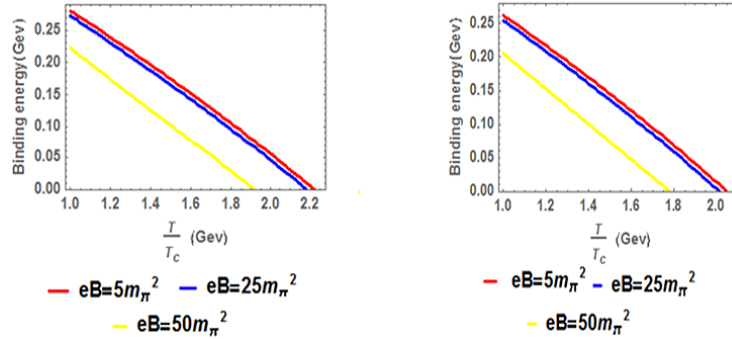
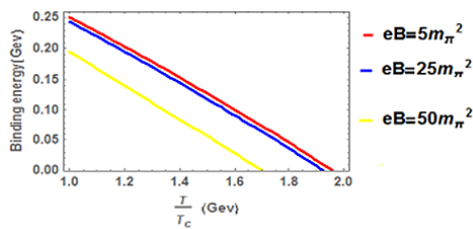


Fig. 7: In the left panel, the Binding energy of charmonium is plotted as a function of T in the thermal medium in presence of eB for the different magnetic field values at $N_f=0$. In the right panel, the Binding energy of charmonium is plotted as a function of the T in the thermal medium in presence of eB for the different magnetic field values at $N_f=2$.



In the lower panel, the Binding energy of charmonium is plotted as a function of T in the thermal medium in the presence of the eB for the different magnetic field values at $N_f=3$.

In Fig.(8), we have plotted binding energy of charmonium at temperature $T=1.98 T_c$, $T=1.99 T_c$ and $T= 2 T_c$ as a function of the magnetic field. We find that BE decreases with the magnetic field increases. By increasing the temperature, we notice binding energy decreases. This conclusion is in agreement with works.^{16, 58}

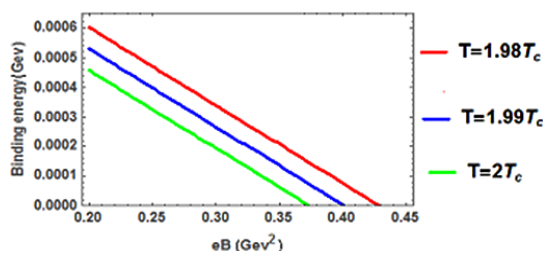


Fig. 8 : The binding energy of charmonium is plotted as a function of magnetic field in the thermal medium for different values of temperature at $N_f=2$.

In Fig.(9), bottomonium binding energy is plotted as a function of T for three cases $eB = 5m_\pi^2$, $eB = 25m_\pi^2$ and $eB=50m_\pi^2$. By increasing the magnetic field, we notice that binding energy of 1S bottomonium decreases. In the upper left panel, we took $N_f = 0$. Besides, the binding energy decreases when taking $N_f = 2$ in the upper right panel. Finally, we find that the BEs decrease with the increase of N_f . At $N_f = 3$, as shown in the lower panel. As a result, we deduce that the N_f plays a role in the decrease of the BE. This finding is in agreement with works.^{16, 50} A similar situation also observed for charmonium, except that the BE for charmonium is higher than that for bottomonium.

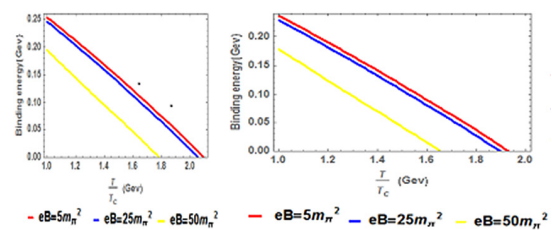
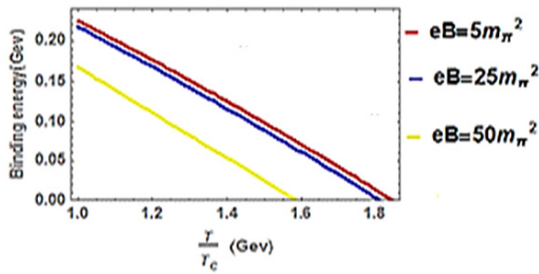


Fig. 9 : In the upper left panel, the Binding energy of bottomonium is plotted as a function of temperature in the thermal medium in presence of magnetic field for different magnetic field values at $N_f=0$. In the upper right panel, the binding energy of bottomonium (in GeV) is plotted as a function of temperature in thermal medium in the presence of magnetic field for the different magnetic field values at $N_f=2$.



In the lower panel, bottomonium Binding energy (in GeV) is plotted as a function of temperature in thermal medium in the presence of magnetic field for the different magnetic field values at $N_f=3$.

In Fig.(10), we have plotted binding energy of bottomonium at temperature $T=1.98 T_c$, $T=1.99 T_c$, and $T=2 T_c$ as a function of the eB . Note that BE with the eB decreases. By increasing the temperature, we notice binding energy decreases. Also, we note that the binding energy tends to zero that depends on the value of the temperature of the medium. This result is noted in Ref.^{16,50}

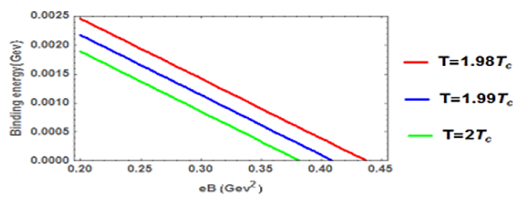


Fig. 10 : The binding energy of bottomonium (in GeV) is plotted as a function of magnetic field in the thermal medium for different values of temperature at $N_f=2$.

Dissociation Temperature for Heavy Quarkonia

Over last two decades, the dissociation of the binding state of the two substances in a thermal medium has improved. When the scan became strong enough, it was expected that the resonance would separate. i.e. prospective is too small to carry $Q\bar{Q}$ pair together. Dissociation is presently thought to be predominantly caused by an increase in the resonance distance, or by Landau damping, an inelastic mechanism of spatially mediated dispersion by a patron such as gluons¹⁴ or because of a process glue-dissociation in which involves hard thermal gluon in one-tone color state.¹⁵ When the medium has lower T than BE of the basic resonance, process become dominant. Thus even at lower temperature, the quarkonium is dissociated even at lower temperatures where likelihood of color processing is small.

The dissociation temperature is calculated in this work at E_b , an approximation that gives worthy accuracy in computation of dissociation temperature. Using the predicted binding energies, we investigate effect of eB on the dissociation temperature for charmonium & bottomonium in presence of hot medium.

In Table (1), the dissociation temperature (T_D) is the minimum when the magnetic field at $eB=50 m_\pi^2$. When $N_f = 0$, the charmonium is dissociated at $2.22 T_c$ when $eB = 5 m_\pi^2$. At the case, $eB = 25 m_\pi^2$ and $eB=50 m_\pi^2$, are dissociated at $2.19 T_c$ and $1.91 T_c$. When $N_f = 2$ charmonium is dissociated at $2.05 T_c$ when $eB=5 m_\pi^2$, in the case, $eB = 25 m_\pi^2$ and $eB = 50 m_\pi^2$, are dissociated at $2.01 T_c$ and $1.77 T_c$. We notice that T_D , in this case is lower compared to $N_f=0$. When $N_f = 3$ charmonium is dissociated at $1.96 T_c$ when $eB=5 m_\pi^2$, in the case, $eB=25 m_\pi^2$ and $eB=50 m_\pi^2$ are dissociated at $1.93 T_c$ and $1.7 T_c$.

Table 1: Dissociation temperature (T_D) for charmonium.

State	$eB=5 m_\pi^2$	$eB=25 m_\pi^2$	$eB=50 m_\pi^2$
$N_f = 0$	$2.22 T_c$	$2.19 T_c$	$1.91 T_c$
$N_f = 2$	$2.05 T_c$	$2.01 T_c$	$1.77 T_c$
$N_f = 3$	$1.96 T_c$	$1.93 T_c$	$1.7 T_c$

In the Table (2), at $N_f=0$ bottomonium is dissociated with $2.1 T_c$ when $eB=5 m_\pi^2$, in the case, $eB=25 m_\pi^2$ and $eB = 50 m_\pi^2$, are dissociated at $2.05 T_c$ and $1.79 T_c$. When $N_f = 2$ bottomonium is dissociated at $1.94 T_c$ when $eB=5 m_\pi^2$, in the case, $eB = 25 m_\pi^2$ and $eB=50 m_\pi^2$, are dissociated at $1.9 T_c$ and $1.65 T_c$. We note that T_D is lower compared to $N_f=0$. When $N_f = 3$ bottomonium is dissociated at $1.85 T_c$ when $eB = 5 m_\pi^2$, in the case, $eB = 25 m_\pi^2$ and $eB = 50 m_\pi^2$, are dissociated at $1.81 T_c$ and $1.59 T_c$. This conclusion is agreed with Ref.^{16,50} In Ref.⁵⁰, In the SE, it is used to the real part of potential and they have found that real part of potential is more screened and by increasing in screening of real part of potential leads to decrease of BEs of Y and J/Ψ . Finally, they got the T_D for Y and J/Ψ , which became slightly lesser in presence of weak magnetic field. At $eB = 0.5 m_\pi^2$ they dissociated at slightly lower value $1.13 T_c$ & $3.94 T_c$. In Ref.¹⁶, the eB influences binding of J/ψ & χ_c . it reduces the binding of J/ψ

but increases the binding of χ_c . In the other hand, the magnetic field raises the width of the resonances because the temperature is too high. We eventually obtained the dissociation due to the Landau damping and noted that the T_D had risen in the presence of a eB . At $eB = 6 m_\pi^2$ the J/ψ is dissociated at $2 T_c$, and with $eB = 4 m_\pi^2$, the χ_c is dissociated at $1.1 T_c$. As the eB increases further the T_D decreases.

Table 2: Dissociation temperature (T_D) for bottomonium.

State	$eB=5 m_\pi^2$	$eB=25 m_\pi^2$	$eB=50 m_\pi^2$
$N_f = 0$	$2.1 T_c$	$2.05 T_c$	$1.79 T_c$
$N_f = 2$	$1.94 T_c$	$1.9 T_c$	$1.65 T_c$
$N_f = 3$	$1.85 T_c$	$1.81 T_c$	$1.59 T_c$

Dissociation of Heavy Quarkonia in a Magnetic Field

We calculate the dissociation of charmonium & bottomonium in magnetic field when $E_b \simeq 0$.

Table 3: Dissociation of charmonium in the magnetic field.

$c\bar{c}$	$T=2 T_c$	$T=1.99 T_c$	$T=1.98 T_c$
	$eB=19.4 m_\pi^2$	$eB=21 m_\pi^2$	$eB=22.57 m_\pi^2$

By taking thermal medium at $T=2 T_c$, we note that the binding energy dissociated as magnetic field increases $eB = 19.4 m_\pi^2$. By decreasing the temperature of the medium up to $T = 1.98 T_c$, we note that the binding energy dissociated at $eB = 22.57 m_\pi^2$. The state of bottomonium is similar to that states of Table (4) but the dissociation of bottomonium is more than of charmonium. This conclusion is agreed with works such that.^{15, 59}

Table. 4. Dissociation of bottomonium in the magnetic field.

$b\bar{b}$	$T=2 T_c$	$T=1.99 T_c$	$T=1.98 T_c$
	$eB=19.95 m_\pi^2$	$eB=21.5 m_\pi^2$	$eB= 23 m_\pi^2$

Summary and Conclusion

We use a generalized m_D that depends on T and eB to find the dissociation of quarkonia in presence

of a strong magnetic field in a hot medium. SE is solved analytically using the NU technique, with the real potential taking into account the finite T and eB effects which are not considered in other works.

We consider the effect of the number of flavors, finite temperature, and magnetic field on binding energy and dissociation temperature. We found that the N_f has a basic role on decreasing binding energy. We have observed that the magnetic field is largely affected by large-distance interaction, as a result of which the real part of potential is more attractive. We report on the results for the values of the magnetic field at $eB = 5 m_\pi^2$, $eB = 25 m_\pi^2$ and $eB = 50 m_\pi^2$. We found the binding energy decreases by increasing the magnetic field. Also, we measure that the T_D is above critical temperature $T_c = 0.17$ GeV, & that T_D of charmonium & bottomonium is lower in a strong magnetic field. This occurs because of the BE decreases by increasing the magnetic field. We note that the T_D decreases with an increase in the N_f and decrease with magnetic field values. We note that the dissociation temperature the of charmonium is greater than that of the bottomonium since the mass of charmonium is smaller than the mass of the bottomonium. This conclusion is agreed with results of Refs.^{16,46,50,59} We hope to include the effect of fractional parameter as a future work.

Acknowledgment

The authors would like to thank Faculty, science, Menoufia University

Funding

There is no funding or financial support for this research work.

Conflict of Interest

Declare there is not the conflict of interest in the manuscript

References

1. J. C. Collins and M. J. Perry, *Phys. Rev. Lett* , 34, (1975) , 1353
2. N. Cabibbo and G. Parisi, *Phys. Lett. B*. 59. (1975), 67–69.
3. I. A. Shovkovy, *Lect. Notes Phys.* 871 (2013), 13
4. M. D: Elia, *Lect. Notes Phys.* 871 (2013), 181
5. K. Fukushima, *Lect. Notes Phys.* 871 (2013), 241.
6. N. Muller, J. A. Bonnet, and C. S. Fisher, *Phys. Rev. D* 89 (2014), 094023.
7. V. A. Miransky and I. A. Shovkovy, *Phys. Rep.* 576 (2015), 1-209.
8. D. Kharzeev, L. McLerran, and H. Warringa, *Nucl. Phys. A* 803 (2008), 227.
9. T. Vachaspati, *Phys. Lett. B* 265 (1991), 258.
10. M. Abu-Shady, *Int. J. Mod. Phys. Appl.* 49 (2018), 1708 .
11. M. Abu-Shady, H. M. Fath-All, *Int. J. Mod. Phys.* 35 (2020), 2050110.
12. M. Abu. Shady, and A. N. Ikot, *Eur. Phys. J. Plus* 134 (2019), 321
13. D. L. Yang and B. Muller, *J. Phys. G* 39 (2012)., 015007 .
14. M. Laine, O. Philipsen, M. Tassler, P. Romatschke, *J. High Energy Phys.* (2007) 03.
15. N. Brambilla, M. A. Escobedo, J. Ghiglieri, A. Vairo, *J. High Energy Phys.* 1305 (2013).
16. M. Hasan, B. K. Patra, P. Bagchi, *Nucl. Phys. A* 955 (2020), 121688 .
17. T. D. Cohen, D.A. McGady, E.S. Werbos, *Phys. Rev. C* 76 (2007), 055201 .
18. J. O. Andersen, *Phys. Rev. D* 86 (2012), 025020.
19. J. O. Andersen, *JHEP*1210 (2012)., 005 .20. S. P. Klevansky, R.H. Lemmer, *Phys. Rev. D* 39 (1989), 3478 .
21. D. P. Menezes, M. Benghi Pinto, S. S. Avancini, C. Providencia, *Phys. Rev. C* 80 (2009)., 065805 .
22. R. Gatto, M. Ruggieri, *Phys. Rev. D* 83 (2011)., 034016
23. R. Gatto, M. Ruggieri, *Phys. Rev. D* 82 (2010)., 054027 .
24. K. Kashiwa, *Phys. Rev. D* 83 (2011)., 117901
25. J. O. Andersen, R. Khan, *Phys. Rev. D* 85, 065026 (2012).
26. S. S. Avancini, D. P. Menezes, M. B. Pinto, and C. Providencia arXiv:1202.5641 (2012).
27. K. Fukushima and J. M. Pawlowski, arXiv:1203.4330 (2012).
28. A. J. Mizher, M.N. Chernodub, E.S. Fraga, *Phys. Rev. D* 82 (2010)., 105016 .
29. J. O. Andersen, A. Tranberg, *JHEP* 08,002 (2012).
30. S. Kanemura, H.-T. Sato, H. Tochimura, *Nucl. Phys. B* 517 (1998), 567.
31. K. G. Klimenko, *Theor. Math. Phys.* 90 (1992), 1.
32. J. Alexandre, K. Farakos, G. Koutsoumbas, *Phys. Rev. D* 63 (2001),065015 .
33. D. D. Scherer, H. Gies, *Phys. Rev. B* 85 (2012), 195417
34. C. V. Johnson, A. Kundu, *JHEP* 12 (2008)., 053
35. F. Preis, A. Rebhan, A. Schmitt, *JHEP* 1103 (2011), 033 .
- [36. A. J. Mizher, E. S. Fraga, M. Chernodub, *PoS FACESQCD* 020 (2010).
37. E. S. Fraga, L. F. Palhares, *Phys. Rev. D* 86 (2012), 016008
38. K. Marasinghe and K. Tuchin, *Phys. Rev. C* 84 (2011)., 044908 .
39. J. Alford and M. Strickland, *Phys. Rev. D* 88 (2013)., 105017 .
40. S. Cho, K. Hattori, S. H. Lee, K. Morita, and S. Ozaki, *Phys. Rev. Lett.*113, 172301(2014).
41. X. Guo, S. Shi, N. Xu, Z. Xu and P. Zhuang, *Phys. Lett. B* 751, 215 (2015).
42. C. Bonati, M. D'Elia and A. Rucci, *Phys. Rev. D* 92, 054014 (2015).
43. R. Rougemont, R. Critelli and J. Noronha, *Phys. Rev. D* 91, 066001 (2015).
44. D. Dudal and T. G. Mertens, *Phys. Rev. D* 91, 086002 (2015).
45. A. V. Sadofyev and Y. Yin, arXiv:1510.06760.
46. M. Hasan, B. Chatterjee, B. K. Patra, *Eur. Phys. J. C* 77, 767 (2017).
47. Af. Nikiforov Uvarov, "Special Functions of Mathematical Physics" Birkhauser, Basel (1988).
48. S. M. Kuchin and N. V. Maksimenko, *Univ. J. Phys. Appl.*7, 295 (2013).
49. R. Kumar and F. Chand, *Commun. Theor. Phys.* 59, 528 (2013).

50. M. Hasan, B. K. Patra, *Phys. Rev. D* 102, 036020 (2020).
51. E. J. Ferrer, V. de la Incera and X. J. Wen, *Phys. Rev. D* 91, 054006 (2015).
52. Yu. A. Simonov, *Phys. At. Nucl.* 58, 107 (1995).
53. M. A. Andreichikov, V. D. Orlovsky and Yu. A. Simonov, *Phys. Rev. Lett.* 110, 162002 (2013).
54. J. Beringer, Particle Data Group, Review of Particle Physics, *Phys. Rev. D* 86, 010001 (2012).
55. V. K. Agotiya, V. Chandra, M. Y. Jamal and I. Nilima, *Phys. Rev. D* 94, 094006 (2016).
56. A. Al-Jamel, *Mod. Phys. Lett. A*, Vol. 34, No. 37, 1950307 (2019).
57. A. Bandyopadhyay, C. A. Islam, M. G. Mustafa, arxiv: 1602.06769V3 (2017).
58. S. A. Khan, B. K. Patra, and M. Hasan, arxiv: 2004.08868V1 (2020).
59. P. Bagchi, N. Dutta, B. Chatterjee, S. P. Adhya, arxiv: 1805.04082V1 (2018).
60. F. Mebarek-Oudina *et al.* *International Journal of Numerical Methods for Heat & Fluid Flow* (2020).
61. S. Marzougui *et al.* *International Journal of Numerical Methods for Heat & Fluid Flow* (2021).
62. P. K. Dadheech *et al.* *Journal of Nanofluids* 9.3 (2020): 161-167.
63. S.M. Abo-Dahab, M.A. Abdelhafez, F. Mebarek-Oudina *et al.* *Indian J. Phys.* (2021). <https://doi.org/10.1007/s12648-020-01923-z>